Available online at www.sciencedirect.com
SCIENCE DIRECT
ELSEVIER
Tectonophysics 416 (2006) 113–131
TECTONOPHYSICS
www.elsevier.com/locate/tecto

Test of the upper mantle low velocity layer in Siberia with surface waves

Antonella Pontevivo *, Hans Thybo

Geological Institute, University of Copenhagen, Øster Voldgade 10, DK-1350 Copenhagen K, Denmark

Accepted 28 November 2005
Available online 27 January 2006

Abstract

The existence of the upper mantle low velocity layer (LVL) below 100 km depth in cratonic areas is tested with surface waves dispersion curves. Given the ambient noise we find that a pronounced LVL (80 km thick and 2% velocity reduction or 40 km thick and 5% velocity reduction) can be distinguished from a constant velocity model by comparison of the fundamental mode group velocities, whereas a thin LVL (less than 40 km thick) with small velocity contrast (less than 2%) cannot be resolved. The fundamental modes of Love and Rayleigh waves have similar properties and, in general, the phase velocity differences are smaller than the standard error. Phase velocity alone cannot discriminate between the models, and the group velocity is in general more sensitive to the velocity structure than the phase velocity. The higher modes at short periods could potentially determine a LVL but in reality it is difficult to obtain sufficiently accurate measurements. We invert the synthetic dispersion curves by the non-linear Hedgehog inversion method. A pronounced LVL (more than 40 km thick and with a strong velocity contrast of about 5%) is detectable by the non-linear inversion but for a thin LVL with a strong velocity contrast it is not possible to resolve both velocity and thickness. In the inversions all solutions include a LVL for models with a pronounced LVL, whereas the solution space includes models with and without a LVL for models with a zero or positive gradient velocity–depth structure.

We invert also real data with travel path across the Siberian craton with the Hedgehog method. Almost all solutions include a LVL in the depth range of 80–150 km with a velocity contrast up to 2% to the surrounding intervals. Hence, the LVL appears to be a common feature of the Siberian upper mantle, although a constant velocity at the same depth range cannot be totally excluded. Despite low resolution at large depth, a pronounced asthenospheric LVL below a depth of about 225 km is a constant characteristic of the set of solutions.

Keywords: Seismic waves; Surface waves; Inverse problems; Dispersion curves; Low velocity layer; Siberian craton

1. Introduction

Surface waves are generally the strongest arrivals at teleseismic distances and provide strong constraints on the vertical velocity variation in the shallow Earth as well as properties of the seismic source. Group and phase dispersion velocities of fundamental modes of both Rayleigh and Love waves are often used to determine the regional seismic velocity structure of the crust and upper mantle. This is particularly useful for the case of a low velocity layer (LVL), for which the inversion of body-wave travel times rarely provides a unique solution. Surface waves do not suffer from the

* Corresponding author. Tel.: +45 35 32 24 81; fax: +45 33 14 83 22.
E-mail address: antonella@geol.ku.dk (A. Pontevivo).

0040-1951/$ - see front matter © 2005 Elsevier B.V. All rights reserved.
doi:10.1016/j.tecto.2005.11.015

same non-uniqueness as body waves in the case of a LVL (van Heijst et al., 1994, and references therein). However, the LVL below approximately 100 km depth beneath a generally stratified mantle may be detectable also in high-density, long-range seismic sections of higher resolution than most other seismological data. From this type of data Thybo and Perchuc (1997) identify a low velocity layer, which further produces strong, scattered reflections beyond 800–900 km (8°) offset.

For the periods of interest for studies of the upper mantle, the group velocities of the higher modes are so close to each other that classical methods of analysis in the time–frequency domain generally cannot be used to separate the different modes. Therefore interpretation of accurate higher mode data requires special tools. Based on studies of the importance of a low velocity channel using higher modes, Panza et al. (1973) and Panza and Calcagnile (1974a,b, 1975) conclude that the higher mode amplitude spectra are useful for discrimination between two types of structures for any focal mechanism. However, in a study of the resolution power of surface waves, Panza (1981) finds that fundamental mode dispersion data are better than higher modes data for resolving the S-wave velocity (v_s) and the thickness (h) of the lithospheric lid.

The first purpose of this study is to investigate if a LVL in the upper mantle is detectable from the dispersion properties of a realistic set of surface waves data calculated with already existing methods. van Heijst et al. (1994) investigate synthetic waveforms as well as phase and group velocities for models with and without a LVL. They find that: (1) For shallow sources, the waveforms cannot discriminate a LVL because shallow sources mainly excite the fundamental mode at short periods, which is not very sensitive to the velocity distribution of the deeper LVL. (2) There are pronounced differences at large propagation distance in the waveform of surface waves propagated through models with different properties for the LVL for sources located in the LVL. However, the generally small differences between the waveforms, the presence of lateral heterogeneity, random noise and errors in source parameters, make it difficult to resolve the differences between the models in a waveform-inversion procedure. (3) The differences between the phase velocities generally are small, both for Rayleigh and Love waves, except for the higher modes at short periods, where the differences exceed the estimated observational error; the group velocities (Rayleigh and Love waves exhibit similar behavior) are in general more sensitive to the velocity of the LVL than the phase velocities. (4) Linear inversion of fundamental mode phase or group velocities alone cannot remove the non-uniqueness of travel time inversions in the presence of a LVL.

Taking into account the results of van Heijst et al. (1994), we calculate the dispersion properties (group and phase velocities of the fundamental and the first few higher modes for both Rayleigh and Love waves) for several types of structures, with and without a LVL in the upper mantle for two depth ranges (100–140 km and 100–180 km of depth) and with velocity reductions of 2% and 5% for the LVL, both in spherical and flat geometry (Fig. 1). We compare the trend of the synthetic dispersion curves for the considered models and we invert the calculated group and phase velocity curves alone and together, using the same structural parameterization and the same period range for each inversion. Instead of using linear inversion as van Heijst et al. (1994), we use the non-linear inversion Hedgehog procedure (Valyus et al., 1969; Valyus, 1972; Knopoff, 1972; Panza, 1981). It searches in a multidimensional parameter space for structures with theoretical dispersion curves, which fall within a given uncertainty of the observations. The most important feature of this non-linear inversion method is its independence from the chosen starting model. The study of a large area (as the Siberian craton) makes it necessary to include the sphericity of the Earth into the calculations, but the existing Hedgehog code for non-linear inversion considers only flat Earth models. Since upgrading of the code to include spherical coordinates is beyond our purposes, we instead take the standard corrections (Muller, 1985) between velocities in the true spherical and the equivalent flat-layered Earth into consideration and demonstrate their validity to the present case.

The synthetic test shows that it is possible to detect the presence of an upper mantle LVL by non-linear inversion of dispersion curves of the fundamental mode of one seismogram. We further carry out joint non-linear inversion of group and phase velocity dispersion curves of Rayleigh waves and we discuss the resolution power of the obtained set of solutions, showing that the LVL probably exists in the upper mantle below the East Siberian craton. Hereby we confirm, by complementary data, the findings from linear inversion of body-wave arrival times by Nielsen et al. (1999) who detect the presence of the LVL in the 100–180 km depth range with a slight P-wave velocity reduction along the 4000 km long PNE (Peaceful Nuclear explosion) profile Kraton in Siberia close to our epicenter-station path. Pavlenkova et al. (2002) also interpret a model of the crust and upper mantle of the Western

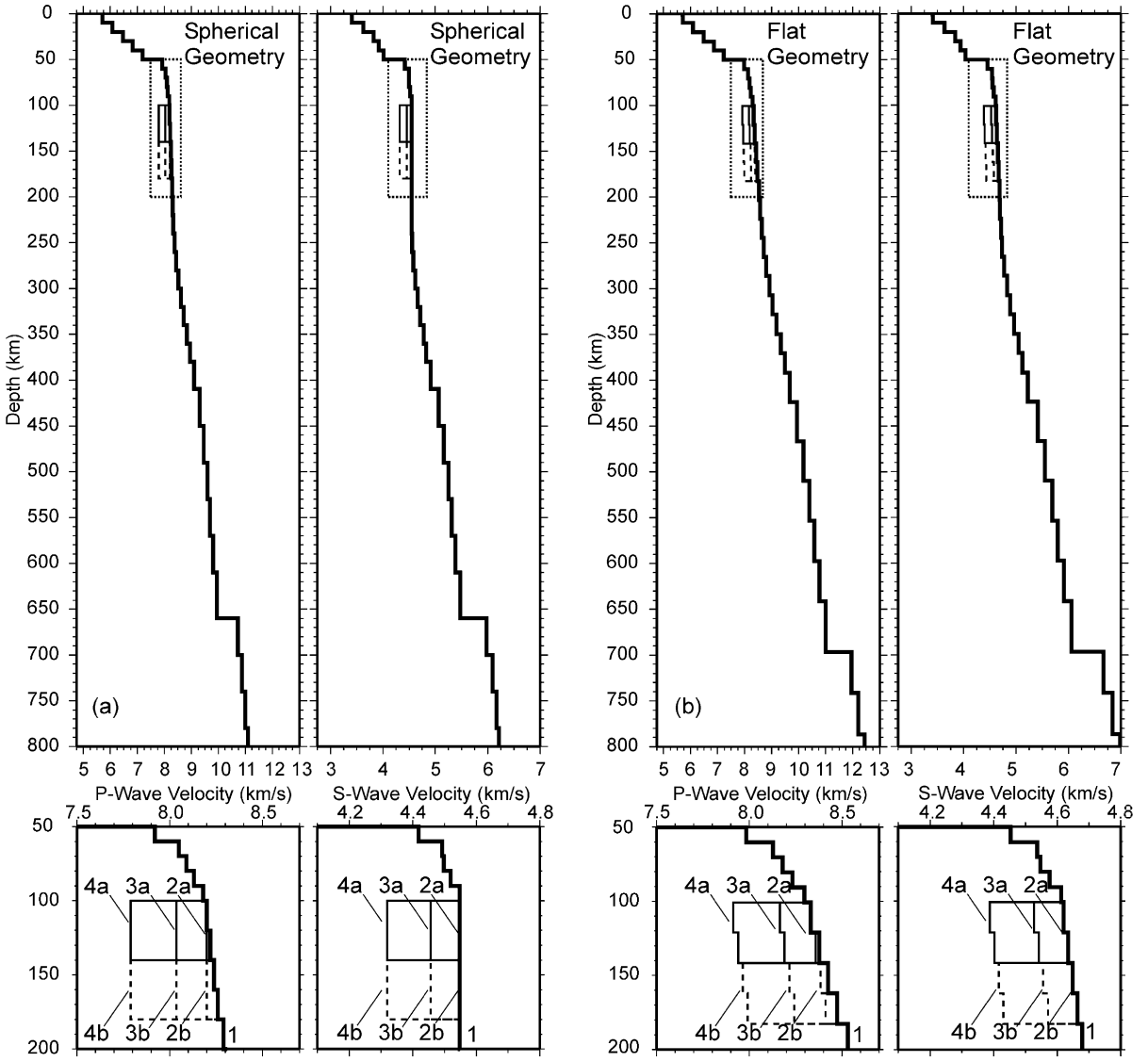

Fig. 1. (Upper part) Seismic velocities v_p and v_s for the considered structural models for the synthetic tests in spherical (a) and flat (b) geometries. Notice the high average velocity compared to global velocity models, e.g. IASP91 (Kennett and Engdahl, 1991). (Lower part) Zoom-in on velocities in the depth range 50–200 km. The v_p of the gradient reference model (the bold line; Mod-1) is a slightly modified version of the model determined by Nielsen et al. (1999). For other models, the reference model is modified in the depth ranges of (a) 100–140 km (the continuous lines) and (b) 100–180 km (the hatched lines): Mod-2 with constant velocity; Mod-3 with $\Delta v(LVL) = -2\%$; Mod-4 with $\Delta v(LVL) = -5\%$.

Siberian craton with a velocity inversion within the lithosphere below about 80 km depth.

However, it is not the intention of this paper to discuss the lateral resolution of multiple paths surface wave tomography methods, which today can be applied to global (e.g. Ritzwoller et al., 2002) and regional studies (Priestley and Debayle, 2003). The latter study shows the existence of lateral variation in S-wave velocity between the Siberian craton and surrounding tectonic areas. This lateral velocity variation is of the same order of magnitude as the vertical variation between the LVL and surrounding layers found in our study. This suggests that the lateral and vertical heterogeneities create velocity anomalies of the same order of magnitude but with much longer wavelength laterally than vertically.

2. The synthetic test: data and method

In the synthetic test we check if the group and phase velocity (v_{gr} and v_{ph}) dispersion curves of the fundamental and the first four higher modes of Rayleigh and

Love waves allow determination of a LVL in the upper mantle below 100 km depth. We investigate two thicknesses (40 km and 80 km) and different velocity reduction (0%, 2% and 5%) of the LVL compared to the surrounding layers (Table 1).

The reference compressional velocity distribution (v_p) is the average 1D-model obtained from body wave tomography along the PNE profile Kraton (Nielsen et al., 1999), where the weak LVL has been substituted by a small positive velocity gradient in the 100–180 km depth interval (Fig. 1). This model takes into account that the average seismic velocity is very high in Siberia. The density is estimated by the Nafe–Drake relation (Ludwig et al., 1970; Fowler, 1995), an empirical relationship between density and seismic velocity (for sedimentary, metamorphic and igneous rocks). The IASP91 model (Kennett and Engdahl, 1991) is used to extend the model down to a depth of 880 km.

The S-wave velocity (v_s) is calculated from the v_p structure through the v_p/v_s ratio of the AK135Q model (Herak et al., 2001). Since the considered v_p/v_s ratio adds an "artificial" low v_s layer between about 150 and 200 km, we have modified the S-wave velocity distribution of the reference model to be constant in the depth interval from 100 to 180 km. This ensures that v_s increases with depth below 180 km (as a consequence, Mod-1 and Mod-2a have the same v_s-distribution but a slightly different v_p-distribution in the depth range of 100–140 km). These models are for true physical parameters of the Earth in spherical geometry (Fig. 1a).

The real Earth differs from a vertically heterogeneous half-space model by its sphericity (e.g. Shearer, 1999). Numerical integration of the equations of motion of a gravitating Earth model by Ben-Menahem and Singh (2000) has shown that: for $T<50$ s, the Earth in flat geometry yields a good approximation; in the period range of 50 s$<T<$300 s, the analysis can be considerably simplified by using a flat-Earth model where the true physical parameters are modified slightly by a suitable Earth-flattening approximation to account for the effects of the sphericity of the Earth. This is in general valid for Rayleigh waves as demonstrated by Bolt and Dorman (1961) who conclude that the combined effect of gravity and sphericity on the phase velocity cannot be ignored for Rayleigh waves with periods larger than about 50 s, whereas group velocities for 100 s$<T<$250 s were accurate to 1%. Another study of mantle Love waves by Kovach and Anderson (1962) demonstrates the importance of the spherical correction for calculations of phase and group velocities for the fundamental and higher modes also at shorter periods. They find that the effect of the sphericity is less extreme but more complicated for fundamental mode Love waves of $T>200$ s than for Rayleigh waves in the presence of a LVL. The explanation may be that the low velocity channel is most effective in trapping energy for Love waves and it therefore makes the effect of sphericity most significant at very short periods. Furthermore the first higher Love mode is more affected by curvature than the fundamental mode. Thus, for the determination of the Earth structure in the presence of the LVL with data for fundamental and higher mode Love waves, the effect of the sphericity must be included even for periods as short as 20 s. Since our purpose is a realistic test of the effects of the LVL over a large area (as the Siberian craton) by comparison of synthetic dispersion curves, we have used the spherical- to flat-Earth correction: (1) the Earth-flattening transformations by Muller (1985) are applied to depth, velocity and density of the spherical-Earth models in order to obtain the corresponding equivalent flat-Earth models (Fig. 1b), which are used for calculation of the dispersion curves; (2) the synthetic phase and group velocity (v_{ph} and v_{gr}) curves of both Rayleigh and Love waves are computed in the equivalent flat-Earth geometry using a computer package by Panza (1985), Panza and Suhadolc (1987), and Florsch et al. (1991).

We have tested the quality of the Earth-flattening transformation applied to our structures by comparing the dispersion curves of the fundamental mode calculated with the Earth-flattening approach and those calculated in spherical geometry with the Fortran code "minos" (Woodhouse, 1988). This code allows calculation of mode frequencies, attenuation, group and phase velocities for a 1D model in spherical geometry (after choosing a group of modes: e.g. spheroidal fundamental, toroidal overtones, radial modes). The two v_{gr} curves show only negligible difference up to periods higher than about

Table 1
Parameters for the interval below 100 km depth for all the considered models (Fig. 1) used for the synthetic studies: (Mod-1) v_p increases with increasing depth; (Mod-2) constant v_p in the depth ranges of 100–140 km (a) or 100–180 km (b); (Mod-3) low velocity layer with $\Delta v_p(LVL)=-2\%$ with respect to the above layer in the depth ranges of 100–140 km (a) or 100–180 km (b); (Mod-4) the same as Mod-3 but with $\Delta v_p(LVL)=-5\%$

Model		Δv_p(LVL) (%)	Depth range (km)
1		Gradient	100–180
2	(a)	0	100–140
	(b)	0	100–180
3	(a)	−2	100–140
	(b)	−2	100–180
4	(a)	−5	100–140
	(b)	−5	100–180

150 s. The differences in the v_{ph} curves increase with the period, starting from about 80 s, but they are not higher than the standard error normally associated to v_{ph} values within the considered period interval. Thus, this test shows that the Earth-flattening approximation is correct in the period interval of interest.

The synthetic dispersion curves of the seven models are compared, within the estimated average error (as suggested by Panza and Calcagnile, 1974a; van Heijst et al., 1994; Shapiro and Ritzwoller, 2002), both in spherical and flat geometry. The non-linear inversion Hedgehog method has been applied to the theoretical v_{gr} and v_{ph} dispersion curves of the seven structures to investigate the uniqueness of the solution space taking into account realistic measurement errors. Main emphasis has been given to the solutions in the 100–250 km depth range.

3. Theoretical dispersion curves

The synthetic dispersion curves (v_{gr} and v_{ph}) of the fundamental and of the first four higher modes (Fig. 2) are computed for both Rayleigh and Love waves and for each of the seven models shown in Fig. 1. The considered error bars follow suggestions in the literature: Panza and Calcagnile (1974a) suggest an error of 0.04 km/s for v_{ph} (as indicated by the experimental v_{ph} determination by Brune and Dorman, 1963), and Panza (1981) proposes an error of 0.06 km/s for v_{gr}.

For all the five lowest orders of Love and Rayleigh modes, the phase velocity (v_{ph}) curves of the seven models are almost similar (Fig. 2a and b). The differences, even if small, increase with increasing difference between the models. The fundamental mode of the gradient structure (Mod-1) has the highest velocity and the other dispersion curves have lower velocity, lowest for the most pronounced LVL (Mod-4b). The differences are mainly in the period range of 50–150 s for the fundamental mode, 20–60 s for the first higher mode, and less than 30 s for the other higher modes. These differences exceed the considered error bars for a pronounced LVL in the fundamental mode case, and there are also large differences for the higher modes at the shortest periods. Since in an experimental case it is difficult to obtain accurate measurements of the v_{ph} of the higher modes for high frequencies, this result suggests that the v_{ph} curves do not allow distinguishing the models in accordance with the result by van Heijst et al. (1994).

In the group velocity (v_{gr}) case, the Rayleigh and Love waves of the models (Fig. 2c and d) show also similar dispersion properties but, since the group velocities are in general more sensitive to the velocity structure than the phase velocities, the differences between the curves are more pronounced than in Fig. 2a and b. The differences are mainly in the period range of 60–180 s for the fundamental mode, for periods less than about 60 s for the first higher mode, and for periods less than about 40 s for the other higher modes. In the case of the fundamental mode it is not possible to make a distinction between models characterized by a gradient, a constant velocity or a weak LVL in the upper mantle within the considered error (between Mods-1, -2, and -3). The difference between models with a pronounced and a weak LVL (Mods-3 and -4) is also weak. However, there are distinct differences between the group velocity curves for models with a gradient velocity (Mod-1) and a thick LVL with strong velocity contrast (Mods-4a and -4b) in the intermediate period range of about 60–180 s. More information may be retrieved from the dispersion curves of the higher modes, in particular at periods shorter than about 40 s where, unfortunately, it is difficult to measure their group velocities since the higher modes cannot be separated easily. This result shows that a pronounced LVL (40 km thick and with a 5% velocity reduction or 80 km thick and 2% velocity reduction) can be distinguished from a gradient model by the group velocity dispersion properties of surface waves.

It is been demonstrated (Kovach and Anderson, 1962) that the higher Love modes are sensitive to upper mantle structure that include a LVL and their dispersion curves are strongly affected by the sphericity, particularly for Earth models including the LVL. Furthermore if accurate deductions are to be made concerning the crust–mantle system using higher Rayleigh modes, the Earth-flattening transformation is satisfactory only for periods less than 25 s (Kovach and Anderson, 1964). Because of these considerations, we perform the non-linear inversion of only the fundamental modes in the following section.

4. Non-linear inversion of the synthetic data

We apply the non-linear inversion Hedgehog method (Valyus et al., 1969; Valyus, 1972; Knopoff, 1972; Panza, 1981) to the synthetic group and phase velocities of the fundamental mode of Rayleigh and Love waves. This inversion method utilizes an optimized Monte Carlo search, such that the solutions are independent of the starting model. The structure is represented by a stack of N homogeneous isotropic elastic layers and each layer is defined by velocities (v_s and v_p), density (ρ) and thickness (h). Each parameter of the structure can be independent, dependent (the parameter has a

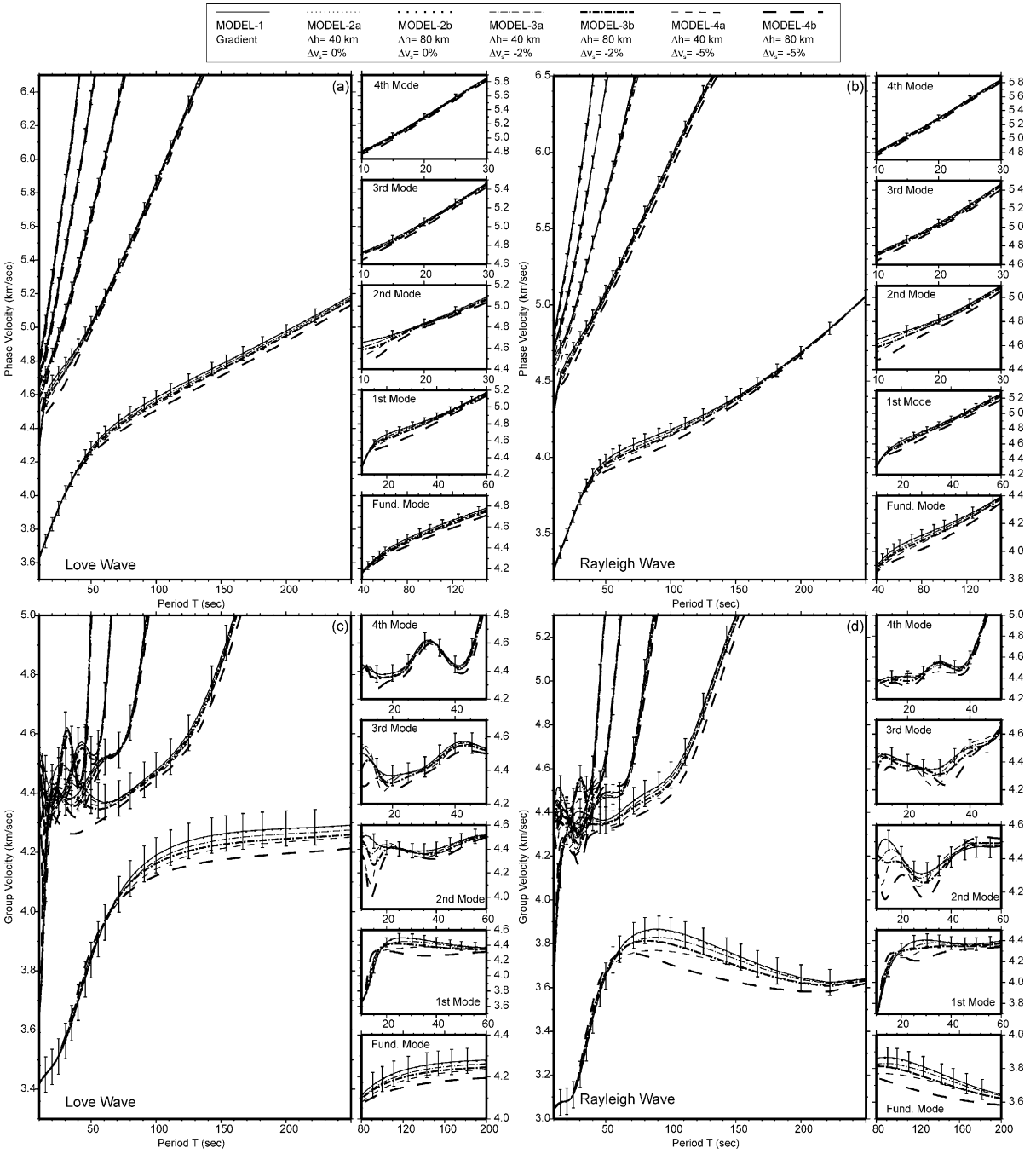

Fig. 2. Dispersion curves of the fundamental and first four higher modes calculated in flat geometry for the considered structures in the period range 10–250 s and at selected periods: a) Love waves v_{ph}; b) Rayleigh waves v_{ph}; c) Love waves v_{gr}; d) Rayleigh waves v_{gr}. The error bars at each period and for all the modes are assumed to be 0.04 km/s for v_{ph} and 0.06 km/s for v_{gr} (Brune and Dorman, 1963; Panza and Calcagnile, 1974a; Panza, 1981; Shapiro and Ritzwoller, 2002). The error bars are centered on the data points calculated for Mod-1.

fixed relationship to another parameter) or fixed. For each structural model, phase and group velocities (v_{ph} and v_{gr}) are computed for the Rayleigh and Love waves. The model is accepted if, at each period, the difference between the computed and the experimental values is less than the uncertainty and if the r.m.s. uncertainty of the differences is less than 70% of the average of the uncertainties (Biswas and Knopoff, 1974; Panza, 1981). In this test the synthetic data are our experimental data. Since the problem is non-unique,

the solution is composed by a set of models (accepted structures) that depends on the parameterization used. The model parameterization may strongly affect the set of solutions and their uncertainties (Shapiro and Ritzwoller, 2002). If the inversion is too weakly constrained, there will be a large number of solutions and large uncertainties will be applied to each depth; tighter constraints on the investigated parameter space reduce the uncertainties but increase the systematic errors of the model. A priori constraints are in general applied to ensure that the selected models are physically plausible.

We apply the same inversion scheme for each model in this synthetic test (Table 2). We limit the inversion to the depth range of 100–245 km, and the used parameterization allows investigation of the thickness h, v_p and v_s of three layers. The v_p/v_s ratio is different for each of the three inverted layers, according to the AK135Q model (Herak et al., 2001). We carry out a test where v_p/v_s is constant and another test with variable v_p/v_s. The variability range of the velocity parameters corresponds to a maximum decrease in velocity of −5% compared to the gradient model. This a priori constraint on the models helps to speed up the computations by limiting the volume of the investigated parameters space and to search physically plausible models. The inversions are performed using thickness and v_s as independent parameters and v_p as dependent parameter, since the surface wave velocities are only weakly dependent on compressional velocities.

In order to minimize the effect of the sphericity of the Earth, we use the dispersion velocities calculated with the "minos" program as input data to the non-linear inversion. Since the Hedgehog method is based on the flat-Earth approximation, the phase velocities are transformed to the flat-Earth case by correcting for the curvature effect with the empirical relation suggested by Bolt and Dorman (1961). No correction is needed for the group velocity since flat- and spherical-Earth group velocity curves differ by negligible amounts.

The synthetic velocity values of both the Rayleigh and Love waves cover the period range of 40–150 s for v_{ph} and of 10–250 s for v_{gr}. These period ranges have been chosen in order to cover the whole period ranges of the real dispersion data described in the next section: from 40 s to 150 s for v_{ph} and from 20 s to 180 s for v_{gr} (Table 3). The period ranges considered in the synthetic test allow to investigate also the crust and the asthenosphere but we focused only on the LVL by inverting for parameters in the depth interval of 100 km to 245 km.

The simultaneous inversion of v_{ph} and v_{gr} provides better constraints to the model than inversion of the phase velocity only. The inversion of v_{ph} eliminates one degree of non-uniqueness, which is inherent in the inversion of v_{gr}. However, v_{gr} information from local earthquakes often provides a useful supplement to v_{ph} information for the inverse problem, since it helps to fix the slopes of the v_{ph} (Knopoff, 1972).

The error for v_{gr} is considered to be equal to 0.06 km/s at each period in the study range. Shapiro and Ritzwoller (2002) use a constant uncertainty of about 0.035 km/s for the Rayleigh waves dispersion maps of v_{ph} but this value reflect only part of the possible errors in the model and not the possible bias in the dispersion maps caused by non-modelled wave-propagation effects such as off-great-circle propagation or scattering. At long periods the spatial resolution is low and, therefore, the resolution of the shear velocity model tends to degrade with depth. Also the discrepancy between the calculation in spherical and flat geometry is larger with increasing period. Hence, the errors for v_{ph} are assumed equal to 0.04 km/s up to 90 s, and slightly larger at the higher periods.

The inversions of the synthetic data have led to the following conclusions:

TEST 1: Using only the calculated v_{gr} of the Rayleigh waves for each model as the experimental data for the inversion, the results show (Fig. 3):
- (a) All solutions include a LVL for dispersion curves of structures with a LVL. For Mod-3a (Fig. 3d) the channel can be 20–60 km thick with a velocity reduction of 2–5%. For Mod-3b (Fig. 3e), the velocity reduction of the LVL ranges from 2% to 5%, with a thickness of 40–80 km. For Mod-4a (Fig. 3f), all the solutions are characterized by a pronounced LVL with thickness of 40–80 km, with at least a sub-layer with $\Delta v_s = -5\%$. In Mod-4b (Fig. 3g), all the solutions include a very thick LVL (80 km or 100 km of thickness) with $\Delta v_s = -5\%$;
- (b) The dispersion curves for structures with a gradient (Mod-1; Fig. 3a) or with a constant layer 40 km or 80 km thick (Mod-2; Fig. 3b and c) primarily leads to solutions that are equivalent to the original model but also to a few structures with a weak LVL in the upper mantle. The LVL solutions include only thin channels (20 km thick) with about $\Delta v_s = -2\%$.

TEST 2: Using the calculated v_{gr} and v_{ph} of the Rayleigh waves for each model as the experimental data for the inversion, there is no differ-

Table 2
Generic parameterization scheme used in the non-linear inversion of the synthetic data for TESTs 1, 2 and 4: h (thickness), v_s and v_p of each layer

h (km)	Model 1		Model 2a		Model 2b		Model 3a		Model 3b		Model 4a		Model 4b	
	v_s (km/s)	v_p (km/s)	v_s (km/s)	v_p (km/s)	v_s (km/s)	v_p (km/s)	v_s (km/s)	v_p (km/s)	v_s (km/s)	v_p (km/s)	v_s (km/s)	v_p (km/s)	v_s (km/s)	v_p (km/s)
Depth < 100	References		References		References		References		References		References		References	
P1	P4	P4 × 1.808	P4	P4 × 1.808	P4	P4 × 1.808	P4	P4 × 1.808	P4	P4 × 1.808	P4	P4 × 1.808	P4	P4 × 1.808
P2	P5	P5 × 1.818	P5	P5 × 1.818	P5	P5 × 1.818	P5	P5 × 1.818	P5	P5 × 1.818	P5	P5 × 1.818	P5	P5 × 1.818
P3	P6	P6 × 1.828	P6	P6 × 1.828	P6	P6 × 1.828	P6	P6 × 1.828	P6	P6 × 1.828	P6	P6 × 1.828	P6	P6 × 1.828
Depth > 245	References		References		References		References		References		References		References	
h (km)	Step (km)	Range (km)	Step (km)	Range (km)	Step (km)	Range (km)	Step (km)	Range (km)	Step (km)	Range (km)	Step (km)	Range (km)	Step (km)	Range (km)
P1	20	20–60	20	20–60	20	20–60	20	20–60	20	20–60	20	20–60	20	20–60
P2	20	20–40	20	20–40	20	20–40	20	20–40	20	20–40	20	20–40	20	20–40
P3	20	20–40	20	20–40	20	20–40	20	20–40	20	20–40	20	20–40	20	20–40
v_s (km/s)	Step (km/s)	Range (km/s)	Step (km/s)	Range (km/s)	Step (km/s)	Range (km/s)	Step (km/s)	Range (km/s)	Step (km/s)	Range (km/s)	Step (km/s)	Range (km/s)	Step (km/s)	Range (km/s)
P4	0.15	4.32–4.62	0.15	4.314–4.764	0.15	4.314–4.764	0.15	4.372–4.672	0.15	4.372–4.672	0.15	4.384–4.684	0.15	4.384–4.684
P5	0.15	4.347–4.647	0.15	4.347–4.647	0.10	4.319–4.719	0.15	4.347–4.647	0.15	4.376–4.676	0.15	4.347–4.647	0.15	4.388–4.688
P6	0.25	4.43–4.68	0.25	4.43–4.68	0.25	4.43–4.68	0.25	4.43–4.68	0.25	4.43–4.68	0.25	4.43–4.68	0.25	4.43–4.68

The uppermost 100 km and the deeper than 245 km part of the structure are fixed based on the reference models (Kennett and Engdahl, 1991; Nielsen et al., 1999). The variable parameters are Pi, with $i = 1, 2, 3$ for thickness and $i = 4, 5, 6$ for v_s. The v_p values are calculated from the v_p/v_s values of the AK135Q model proposed by Herak et al. (2001). The step and the variability range of each parameter Pi are also shown. The velocity ranges are introduced in order to keep the minimum velocity contrast above − 5% and the maximum value close to the gradient model values. In TEST 4 also the v_p/v_s of the first two investigated layers are considered as independent parameters of the inversion.

Table 3
Real data group (v_{gr}) and phase (v_{ph}) velocity values at periods from 20 s to 180 s and from 40 s to 150 s, respectively, with the single point error (ρ_{gr}, ρ_{ph}) and the r.m.s. values

Period (s)	v_{gr} (km/s)	ρ_{gr} (km/s)	v_{ph} (km/s)	ρ_{ph} (km/s)
20	2.97	0.06		
25	3.14	0.075		
30	3.34	0.075		
35	3.50	0.06		
40	3.61	0.06	3.91	0.04
45	3.69	0.06		
50	3.75	0.06	3.97	0.04
60	3.82	0.06	4.01	0.04
70	3.84	0.06	4.03	0.04
80	3.85	0.06	4.05	0.04
90	3.85	0.06	4.08	0.04
100	3.85	0.06	4.10	0.05
120	3.83	0.14		
125			4.16	0.05
140	3.80	0.23		
150			4.24	0.06
160	3.80	0.30		
180	3.83	0.33		
r.m.s.		0.076		0.035

The phase velocities are corrected for sphericity following Bolt and Dorman (1961).

ence in the solution space to the case of inverting both the Rayleigh and Love waves together (Fig. 4). The results are very similar to TEST 1 but the number of solutions is smaller.

(a) The inversions of dispersion curves of structures with a LVL (Mod-3 and Mod-4; Fig. 4d–g) lead only to solutions that include a LVL. The solution space changes with the considered original model and there is a trade-off between the thickness of the LVL and the velocity reduction;

(b) The inversions of dispersion curves for structures with a gradient (Mod-1; Fig. 4a) or with a constant layer 40 km or 80 km thick (Mod-2; Fig. 4b and c) primarily leads to similar solutions but also structures with a LVL in the upper mantle are solutions. However, where it is present, the LVL is less than 20 km thick with $\Delta v_s < -2\%$.

TEST 3: Using the calculated v_{gr} and v_{ph} of the Rayleigh waves for models with a LVL with different decrease in v_s and v_p (low v_p/v_s: $\Delta v_s = -2\%$ and $\Delta v_p = -5\%$; high v_p/v_s: $\Delta v_s = -5\%$ and $\Delta v_p = -2\%$) as the experimental data for the inversion, the results show that only models with a LVL in the upper mantle are solutions:

(a) Low v_p/v_s leads to structures (Fig. 5a and b) with a LVL that may be pronounced or weak;

(b) High v_p/v_s leads to structures (Fig. 5c and d) with a very pronounced LVL (always about $\Delta v_s = -5\%$) and with a thickness that can be very large (>60 km).

Thus using a different percentage deviation for v_p and v_s does not affect the possibilities of determining the presence of the LVL by inversion of dispersion curves.

TEST 4: We use v_{gr} and v_{ph} of the Rayleigh waves for the models with a LVL (Mod-3 and Mod-4) as experimental data for the inversions and accept variable v_p/v_s ratios in the parameterization. The number of solutions (not shown) is very large (more than 60). The results show that the inversion for v_p/v_s ratios does not change the results otherwise obtained and all solutions include a LVL:

(a) A LVL with $\Delta v_s = -5\%$ (Mod-4) leads only to solutions with $\Delta v_s = -5\%$ and a thick LVL;

(b) A LVL with $\Delta v_s = -2\%$ (Mod-3) leads to solutions with variable types of LVL. The LVL is never both pronounced and thick for the same model.

5. Inversion of dispersion curves from Siberia

To investigate the existence of a LVL in the Siberian Craton, we use data recorded at the Zerenda station (ZRN) in Kazakhstan from the 1994 earthquake in the southern part of the Kamchatka Peninsula (Fig. 6). This epicenter-station path crosses the West Siberian Platform, the older Siberian craton and the orogenic area of Kamchatka. The frequency–time analysis, FTAN, (Levshin et al., 1972, 1992, 1994) is applied to the waveform to extract the group velocity dispersion curve of the fundamental mode of the vertical (Rayleigh waves) component (Fig. 7). Due to the large epicenter-station distance and the considered period range for v_{gr} between 20 s and 180 s, the error due to the source is negligible and already included in the estimated experimental error that we consider. Comparison of the selected curve with the group velocity dispersion curves of other data across the study area (Fig. 7) and extracted using the same method of frequency–time analysis, shows a similar trend in the whole considered period range. This justifies our choice of considering only the

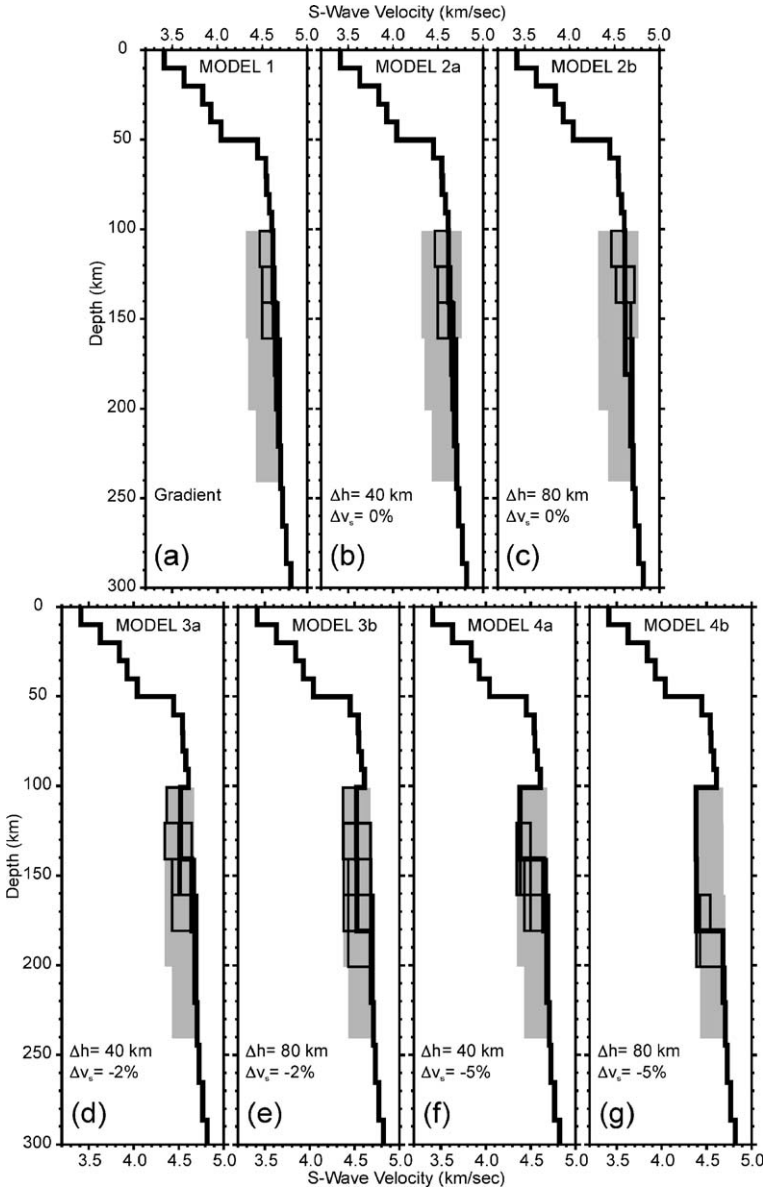

Fig. 3. (TEST 1) Sets of solutions (v_s versus depth) for the inversions of only the calculated v_{gr} for Rayleigh waves of the various models as experimental data. The grey areas represent the investigated parameter space; the black lines are the solutions; the bold line is the Model of Fig. 1 for which the dispersion curve is calculated to be used in the inversion. Hence, it is also a solution of the set.

data of one epicenter-station path, i.e. the one with the deepest hypocenter, which should provide the optimum data on the LVL according to van Heijst et al. (1994), who demonstrate that the waveforms are mainly affected by details of the LVL when the source is located at a depth near the LVL. As such the related dispersion curve provides the best option for testing the possible existence of a LVL and defining an average structure of the region. The v_{gr} uncertainty is experimentally estimated, from the difference in the velocity values determined along similar paths across similar areas, to be 0.06 km/s in the period range 20–90 s (except 0.075 km/s at 25 s and 30 s) and between 0.06 km/s and 0.33 km/s for periods higher than 100 s (Table 3 and Fig. 7). The largest errors are due to the ambiguity of the identification of the fundamental mode at the higher periods. Therefore, to allow better constraints on the inversion at high periods, we find it important to use also phase velocity dispersion data, even though the synthetic test has demonstrated that the phase velocity is of secondary importance for discrimination of the LVL.

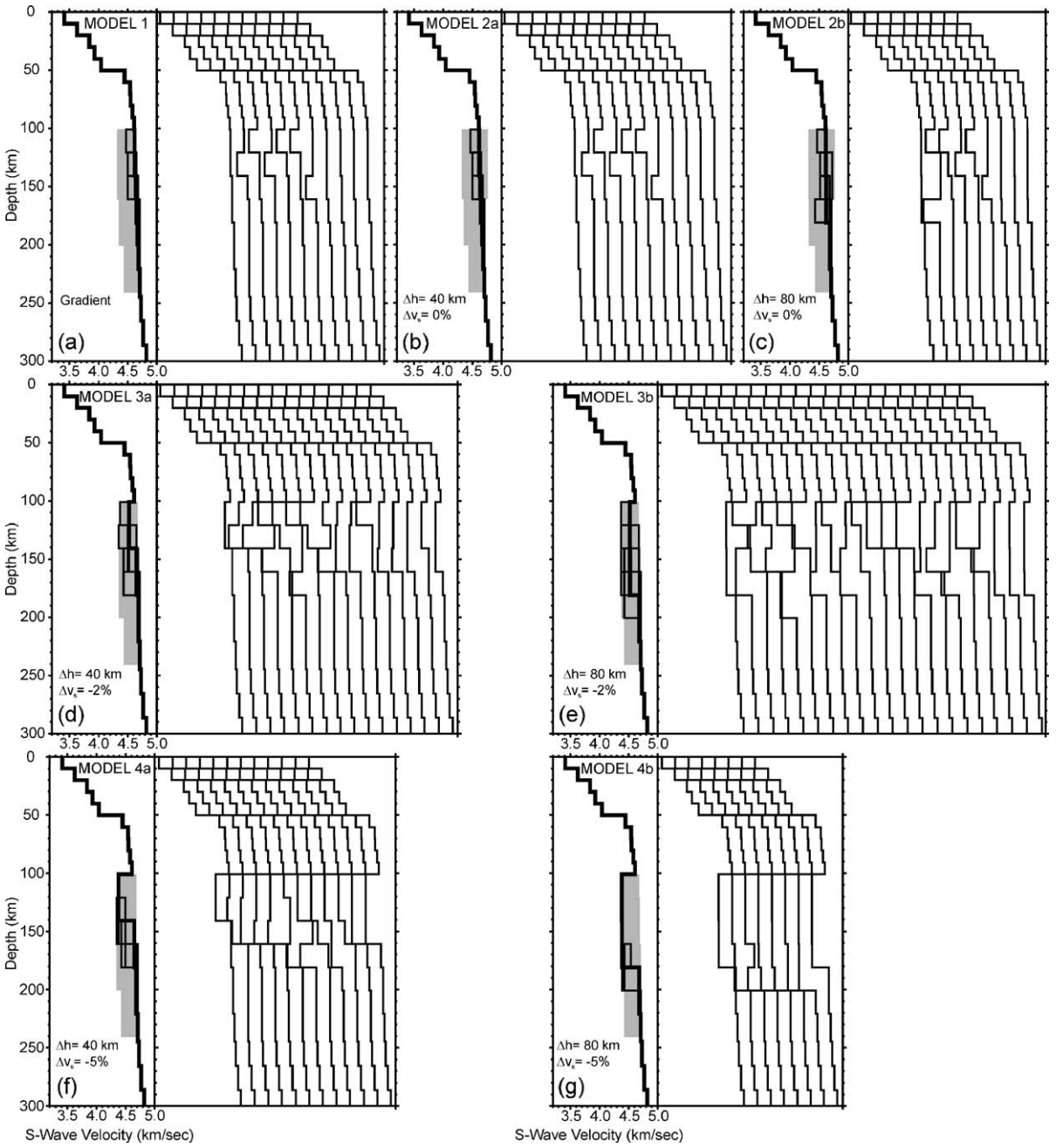

Fig. 4. (TEST 2) For each model: on the left, set of solutions (v_s versus depth) for the inversion of the calculated v_{gr} and v_{ph} for Rayleigh and Love waves of the model as experimental data; on the right, all the v_s solutions are plotted one by one. The grey areas represent the investigated parameter space; the black lines are the solutions; the bold line is the Model of Fig. 1 for which the dispersion curve is calculated to be used in the inversion.

The average phase velocity dispersion curve of the Rayleigh waves is extracted from the diffraction tomography maps by Shapiro and Ritzwoller (2002), who analyzed data sets of Trampert and Woodhouse (1995) and Ekstrom et al. (1997) with the method by Ritzwoller et al. (2002). The average v_{ph} is calculated from $1^\circ \times 1^\circ$ cell data in a band along the considered epicenter-station path in the period range 40–150 s. The measurement error of the phase velocity (see previous section) is fixed to the value of 0.04 km/s up to 90 s, and between 0.05 and 0.06 km/s at higher periods (Table 3 and Fig. 8b). The r.m.s. uncertainty of v_{gr} and v_{ph} is estimated to be about the 70% of the average value of the errors.

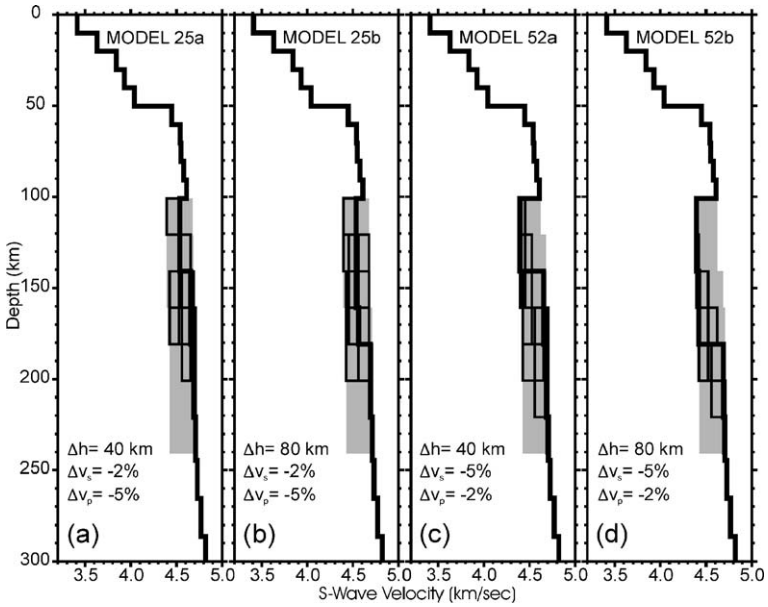

Fig. 5. (TEST 3) Sets of solutions (v_s versus depth) for the inversions of the calculated v_{gr} and v_{ph} for Rayleigh waves of the various models characterized by: (a, b) $\Delta v_s(LVL) = -2\%$ and $\Delta v_p(LVL) = -5\%$ (low v_p/v_s, called Mod-25); (c, d) $\Delta v_s(LVL) = -5\%$ and $\Delta v_p(LVL) = -2\%$ (high v_p/v_s, called Mod-52). The grey areas represent the investigated parameter space; the black lines are the solutions; the bold line is the input structure for calculation of the synthetic data.

The non-linear inversion Hedgehog method is applied to joint inversion of the v_{gr} and v_{ph} dispersion curves of the real data. Independent geophysical information available from the literature (Egorkin, 1991; Yanovskaya et al., 2000; Yanovskaya and Kozhevnikov, 2003) is used to fix the velocity profile of the crustal layers (the uppermost 40 km) in order to improve the resolution of the inversion. The structure deeper than 371 km is fixed based on reference models (Kennett and Engdahl, 1991; Nielsen et al., 1999).

In order to determine the depth range that is constrained by the data (and therefore should be included in the parameterization for the inversion), we calculate the partial derivatives (Rodi et al., 1975; Urban et al., 1993) of the dispersion curves with respect to the considered parameters for a hypothetical structure at all the periods of the experimental data. This shows that the phase and group velocities in the whole period range from 20 s to 180 s are influenced by the seismic velocities and thicknesses of the layers in the depth

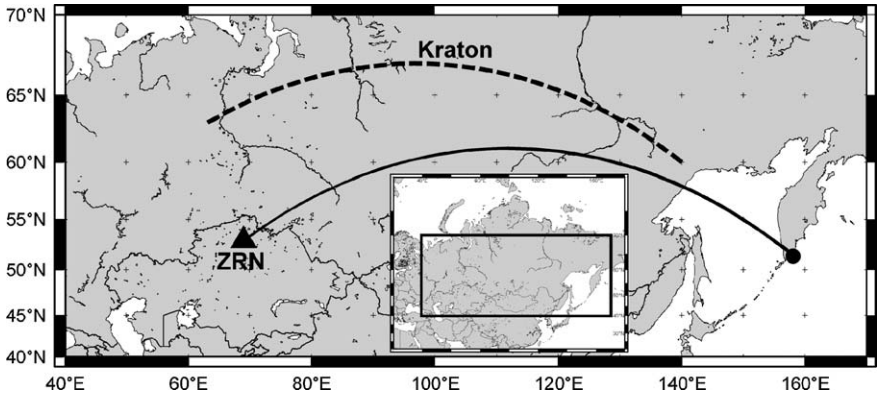

Fig. 6. The epicenter-station path (black line) of the real data in the Siberian study area. The Zerenda station (ZRN) in Kazakhstan (triangle) and the epicenter (circle) of the event (14:17:52.10 – 02/08/1994; 145 km depth; MB = 6.0) in the southern part of the Kamchatka Peninsula are shown. The stippled line represents the PNE (Peaceful Nuclear Explosion) profile Kraton along which the mantle LVL has been demonstrated by tomographic inversion of explosion seismic data (Nielsen et al., 1999).

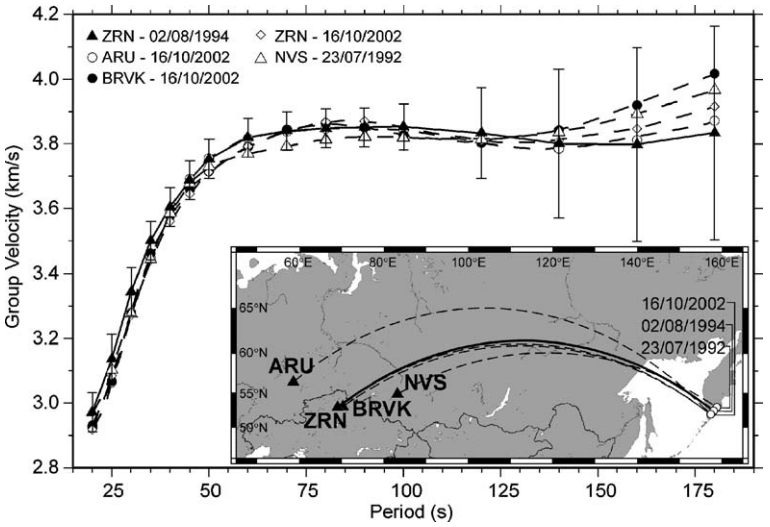

Fig. 7. Rayleigh wave group velocity dispersion curves, extracted by FTAN, of the data whose epicenter-station paths are shown in the frame. By continuum line and black triangles is indicated the v_{gr} curve of the experimental data (event 02/08/1994 recorded by ZRN, Zerenda) with the corresponding error bars used in the inversion. The hatched lines indicate the data used for the comparison: event 23/07/1992 recorded by NVS (Novosibirsk); event 16/10/2002 recorded by ARU (Arti), BRVK (Borovoye) and ZRN (Zerenda).

range between about 40 and 370 km, where we invert for h, v_p and v_s in five layers (Table 4). The v_p/v_s ratios of the layers are different but they are kept constant in the inversion. The upper limit of the v_s is fixed at 4.8 km/s and the lower limit between 4.0 and 4.2 km/s for the LVL at depths greater than about 60 km. We show the set of solutions resulting from the inversion to 450 km depth although the models are mainly resolved to about 250 km depth (Fig. 8a).

The single path dispersion measurements sample mainly the Siberian craton together with parts of the tectonically younger parts of Siberia at the eastern end of the profile. Therefore, the inversion result is the average structure of all the tectonic elements crossed by the path. Other studies have shown that the lateral variation in seismic velocity along the study paths (Priestley and Debayle, 2003) is on the same order as the variation between the LVL and surrounding layers in this study. We therefore can be confident that the vertical velocity profile found by our method is representative of the upper mantle along the travel path between source and seismograph. Further, the results from inversion of body-wave travel times along the almost coincident PNE profile Kraton (Nielsen et al., 1999; Fig. 6) shows stronger vertical than lateral variation in seismic velocity.

The depth of the Moho for all the structures is about 40 km. Almost all solutions (14 of 17) include a LVL in the uppermost mantle but two solutions have a zero and one solution has a positive gradient layer in the 40–130 km depth range.

The models with a LVL are characterized by a mantle lid (20–40 km thick) with v_s about 4.5 km/s, above the LVL (with v_s about 4.35–4.45 km/s) generally at a depth of 75 km to 150 km, centered at a depth of about 110 km. The deep structure is characterized by v_s of about 4.6–4.8 km/s above an asthenospheric low velocity channel (v_s about 4.2–4.4 km/s) below 200–225 km depth. For the three solutions with a zero or positive gradient layer below the Moho, the v_s increases with depth from 4.4 to 4.8 km/s, down to about 250 km, which is the depth to the asthenospheric channel with v_s about 4.2–4.4 km/s. Thus, a low velocity asthenospheric layer is common to all solutions. However, it is not well resolved by the data that loose the resolving power below a depth of 250 km.

The average structure (the bold line in Fig. 8a) is computed from all the solutions of the set as the mean velocity inside each layer, delimited between two discontinuities. It includes the Moho at about 40 km depth above a 40 km thick lid with v_s about 4.5 km/s; a weak LVL below about 80 km depth with a thickness of 70 km and $4.40 \le v_s \le 4.45$ km/s; a high velocity and positive gradient below about 150 km depth above an asthenospheric low velocity layer below a depth of 225 km with v_s~4.25 km/s. This average model is not a solution of the set but it is close to the solution No. 2 (Fig. 8a), which also corresponds to r.m.s. uncertainties of v_{gr} and v_{ph} close to the average values.

The lower asthenospheric LVL has not been introduced in the a priori model but it is a pure result of the inversion of the experimental data. We tested the ro-

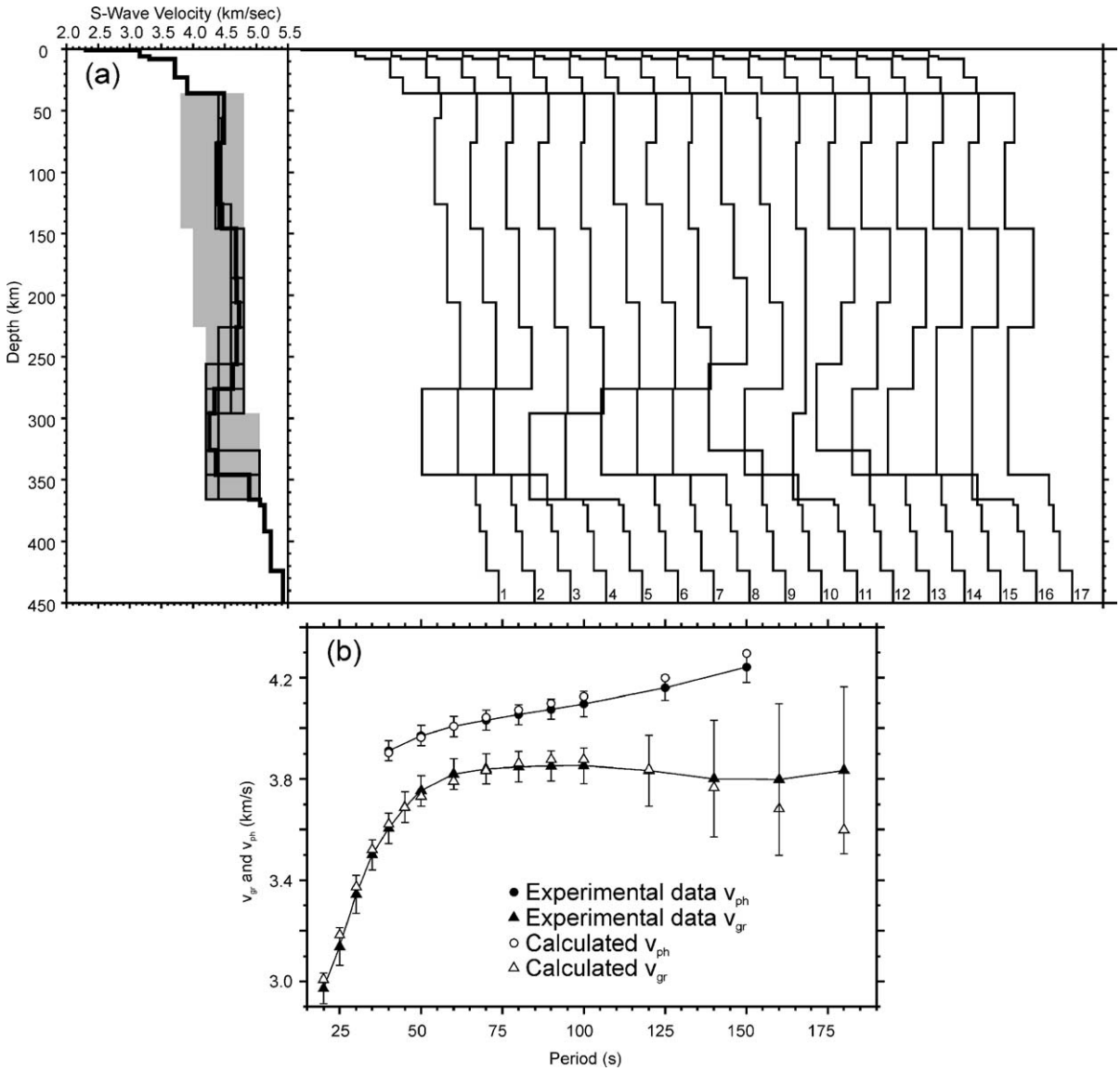

Fig. 8. (a) On the left, the set of solutions (v_s versus depth) for the inversion of real data shown as dispersion curves in (b). The grey area represents the investigated parameter space; the black lines are the solutions; the bold line is the average structure calculated from all the solutions of the set. On the right, the solutions are plotted one by one. (b) Rayleigh waves dispersion curves v_{gr} and v_{ph} of the experimental data used in the inversion with the corresponding error bars, together with the velocities calculated for the solution No. 2 of the set resulting from the inversion.

bustness of this feature by running the inversion with a fixed structure deeper than 200 km (and 250 km). The result shows that no solution can be found unless the deep structure includes the asthenospheric channel. Further, forcing the deep fixed structure to include the low velocity asthenospheric layer, almost all the solutions include an upper mantle LVL.

To further discriminate between the structures of the set in order to select the most representative model, we have calculated the correlation coefficient between the calculated dispersion curve of each solution of the inversion and the real data for both the group and the phase velocities. The correlation coefficient potentially provides information on the quality of the least squares fit to the original data. In our calculations the minimum value of the coefficient is 0.9217 for the group velocity and 0.9957 for the phase velocity, which means that the calculated dispersion curves fit the real data. The best combination of the coefficients for the group and the phase velocities is associated with solution No. 5, which is characterized by the presence of a LVL (Fig. 8a). Solutions Nos. 2 and 4

Table 4
Parameterization and obtained solutions in the non-linear inversion of real data

(a)

h (km)	v_s (km/s)	v_p (km/s)
1	2.30	4.00
5	3.15	5.40
2	3.30	5.65
15	3.70	6.49
13	3.90	6.86
P1	P6	P6 × 1.804
P2	P7	P7 × 1.804
P3	P8	P8 × 1.800
P4	P9	P9 × 1.808
P5	P10	P10 × 1.828
Depth > 371	References	References

(b)

Step	20	20	20	20	20	0.10	0.05	0.20	0.20	0.20		
Range	20–40	10–70	20–80	30–70	30–70	3.8–4.8	3.8–4.8	4.0–4.8	4.2–4.8	4.2–4.8		
Initial value	40	70	80	70	70	4.5	4.4	4.6	4.8	4.2		
No.	P1, h (km)	P2, h (km)	P3, h (km)	P4, h (km)	P5, h (km)	P6, v_s (km/s)	P7, v_s (km/s)	P8, v_s (km/s)	P9, v_s (km/s)	P10, v_s (km/s)	r.m.s., v_{ph} (km/s)	r.m.s., v_{gr} (km/s)
1	−1	0	0	0	0	0	0	0	0	0	0.025	0.070
2	0	0	−1	0	0	0	0	0	0	0	0.027	0.070
3	0	0	0	−1	0	0	0	0	0	0	0.019	0.075
4	0	0	0	0	0	0	−1	0	0	0	0.019	0.073
5	0	0	0	0	0	0	1	0	0	0	0.032	0.065
6	−1	0	0	0	0	−1	0	0	0	0	0.024	0.073
7	0	−1	0	0	0	0	−1	0	0	0	0.031	0.069
8	0	0	0	−1	0	0	1	0	0	0	0.028	0.072
9	−1	0	−1	0	0	−1	0	0	0	0	0.029	0.076
10	−1	0	0	0	0	−1	1	0	0	0	0.030	0.069
11	0	0	0	0	0	0	1	0	−1	1	0.025	0.073
12	0	0	−1	−1	0	0	0	1	−1	0	0.033	0.076
13	0	0	−1	0	0	0	−1	1	−1	0	0.022	0.076
14	0	0	0	−1	0	0	−1	1	−1	0	0.029	0.072
15	0	0	0	−1	0	0	−1	1	−2	1	0.029	0.075
16	0	0	0	0	0	0	−1	1	−2	1	0.020	0.076
17	0	0	0	0	−1	0	−1	1	−2	1	0.029	0.075

(a) h (thickness), v_s and v_p of each layer. The crustal layers are fixed based on the available literature (Egorkin, 1991; Yanovskaya and Kozhevnikov, 2003) as well as the structure deeper than 371 km (Kennett and Engdahl, 1991; Nielsen et al., 1999). The variable parameters are Pi, with $i = 1, \ldots, 5$ for thickness and $i = 6, \ldots, 10$ for v_s. (b) Step, variability range and initial value of each parameter Pi are shown (the uppermost three lines). The non-linear inversion solutions are presented (lower part): the number of steps to add or to subtract (to the initial value) for each parameter is indicated in order to build the model. The respective r.m.s. values of the solutions are shown on the right.

(Fig. 8a), together with one of the three solutions (solution No. 6) with a zero or positive gradient layer in the upper mantle, fall in a group of solutions with large correlation coefficients.

We have also tested whether the dispersion curves calculated for each of the models in the set of solutions should show a constant bias compared to the data dispersion curves. We calculate the bias coefficient as the mean residual taking into account the sign. A constant bias (synthetic group or phase velocities always higher or lower than the data velocities) would indicate that the model generally has too high or too low velocity and, therefore, should be disregarded in the set of solutions. We find that the solutions with a constant velocity (Nos. 6 and 9) and a positive gradient (No. 10) as well as solution No. 5 (weak LVL) all show a tendency towards a constant bias. The calculated bias coefficient for these models is around $8–12 \times 10^{-4}$. On the contrary, solutions Nos. 2 and 4 show the smallest bias coefficient ($\sim 4 \times 10^{-4}$) of all models, i.e. the calculated dispersion velocities are distributed in a random way around the data curve.

Given that all except three solutions (which all show a systematic bias) include a LVL in the depth interval from 80 to 150 km and the experience from the synthetic test, the non-linear inversion results show that the upper mantle low velocity layer most probably exists in Eastern Siberia.

6. Discussion and conclusions

The dispersion curves of the higher modes at short periods potentially could provide information on the structural properties of the upper mantle and allow identification of a LVL, but it is difficult to obtain accurate measurements of these group and phase velocities. Considering only the fundamental mode, Love and Rayleigh waves have similar properties and, in general, the phase velocity differences are smaller than the standard error, as also found by van Heijst et al. (1994). It is clear that phase velocities alone cannot discriminate between the models, unless the experimental error could be significantly reduced. Group velocities are in general more sensitive to the velocity structure than phase velocities. The group velocity dispersion characteristics of the fundamental mode represent the only possibility to distinguish between models characterized by a positive velocity gradient and a LVL in the upper mantle as well as to determine the seismic properties of such a channel. We find that the differences in fundamental mode dispersion characteristics, even if small, increase with increasing difference between the models in the intermediate period range of about 60–180 s for both Rayleigh and Love waves. The fundamental mode for the gradient structure has the highest velocity and the other dispersion curves are all slower, slowest for the most pronounced LVL. The result shows that it is not possible to distinguish, within the considered error, neither between models characterized by a gradient and a weakly developed LVL in the upper mantle, nor between models with a pronounced and a weak LVL. However, the group velocity curves are distinctly different for models with a constant velocity and a thick LVL with strong velocity contrast to the surrounding depth intervals such that it is possible to detect a pronounced LVL.

Our results generally confirm the results of the surface waves study by van Heijst et al. (1994) regarding the possibility of detecting the presence of the low velocity layer. They demonstrate that linear inversion of only the fundamental mode cannot resolve the LVL, neither for the phase nor the group velocities. They conclude that the resolving power of a linear inversion based on only the fundamental mode is too small. On the contrary, our results obtained from non-linear inversion of synthetic dispersion data of the fundamental mode, allow us to state that:

(a) A LVL in the upper mantle that is more than 40 km thick with a strong velocity contrast of about 5% is detectable by non-linear inversion of surface wave dispersion curves of the fundamental mode. However, one cannot resolve both velocity and thickness independently for a thin LVL with a strong velocity contrast since several different models give a good data fit;
(b) The inversions of dispersion curves for models with a weak LVL, thin or thick, lead only to models with a LVL but with unconstrained seismic properties. Thus, a LVL is likely present if all results of inversion of a real data set include a LVL with large variety in properties of velocity and thickness;
(c) From the inversion of fundamental mode dispersion curves we cannot uniquely discriminate between models with a weak LVL (less than 40 km thick and 2% velocity contrast) and a constant or a gradient layer in the upper mantle. The results show that inversions of dispersion curves for structures with a zero or positive gradient may also include a few structures with a weak LVL in the upper mantle.

The non-linear inversion of the real data from the East Siberia craton leads to a set of solutions comparable with those obtained from the test of models with a weak LVL (Δv less than 2%) in the upper mantle: almost all solutions of the inversion include a LVL with v_s about 4.35–4.45 km/s in the depth range of about 80–150 km; but three out of 17 solutions are characterized by a zero or positive gradient layer down to about 250 km. Therefore, the LVL is not a pronounced feature of the upper mantle in eastern Siberia, but a weak LVL is probably present with a velocity contrast of less than 2% with respect to the velocity value of the uppermost lid and with a thickness up to 70 km. From a mathematical point of view, the most representative structure includes the LVL, considering the correlation coefficient and the bias with the data as well as the average structure calculated from the full set of solutions. The presence of the LVL is in agreement with the results of tomographic inversion of data from the PNE profile Kraton (cf. Fig. 6) across the Siberian platform by Nielsen et al. (1999). Their study demonstrates the presence of the LVL in the 100–180 km

depth range with a velocity reduction of <2% compared to the background model.

The presence of a weak LVL at a depth of about 100–150 km is also in agreement with the 2-D model of the crust and upper mantle for the Western Siberian craton proposed by Pavlenkova et al. (2002) based on ray tracing techniques. In their model from travel time modelling of recordings from chemical and nuclear explosions, Pavlenkova et al. (2002) found a velocity inversion below a depth of about 80 km within the lithosphere, with a strong reflecting interface at its base. It may be significant that three independent methods have found similar values for both the velocity and the depth range of the LVL and as well as the structure below and above the LVL.

Priestley and Debayle (2003) present an S_v-wavespeed tomographic model in the form of horizontal slices and vertical cross-sections based on fundamental and higher mode regional waveforms data set from Siberia. However, the model does not resolve the wavespeed above 100 km depth and, therefore, it cannot identify the LVL in the upper mantle. Their main result is a pronounced and abrupt division between high wavespeed beneath the stable region of north-central Asia and low wavespeed beneath the back arc basins to the west of the Kamchatka, Kuriles and Japan volcanic arc. Their inversion approach is designed to identify mainly lateral variation in wavespeed, such that the vertical variation in their model depends strongly on the background and input models, as there is a trade off between the obtainable horizontal and vertical resolution in surface wave inversion. The lateral variability in wavespeed found by their study is of the same order of the vertical variation found in our model. Hence, one may conclude that both models show significant, well resolved results and, as such, both lateral and vertical variation in wavespeed exist, including the upper mantle low velocity layer and a sharp transition between the shield and surrounding areas.

Pavlenkova et al. (2002) interpret reflectors within the upper mantle at depths between 230 and 350 km, suggesting the presence of a deeper LVL, which may be interpreted as a low velocity asthenospheric layer in agreement with our results of the non-linear inversion. In addition, Priestley and Debayle (2003) estimate the upper mantle lid base to lie between 175 km and 225 km depth beneath most of the Siberian platform. However they also find that a thicker lithosphere may exist beneath small and isolated areas, which is in partial agreement with the results by Artemieva and Mooney (2001), who find the thermal lithosphere beneath parts of the Siberian platform to be about 350 km thick.

Hales (1991), Pavlenkova (1996), Perchuc and Thybo (1996) and Thybo and Perchuc (1997) all suggest that a weak LVL at a depth of about 100–160 km may be explained by the existence of partial melt. Such a layer in Fennoscandia shows strong attenuation of seismic waves, in particular S-waves (Abramovitz et al., 2002), and generates scattered reflections in the seismic data (Nielsen et al., 2002). From a thermal and petrological point of view, Thybo and Perchuc (1997) propose that the LVL may contain carbonatic and kimberlitic partial melt in separate bodies of relatively small lateral extent (<20 km), causing both the scattered reflections and low velocities. Although the layer may contain partially molten inclusions, it is only necessary that it has a temperature close to the solidus to explain the low velocity and its characteristic scattering properties (Nielsen et al., 2001). Sato et al. (1989) show that significant velocity reduction occurs at temperatures above 80% of the solidus temperature. The heat flow estimated temperature of the mantle in Siberia (Artemieva and Mooney, 2001) indicates that the temperature of rocks below ca. 100 km depth is within 80–100% of the solidus, provided that sufficient amounts of volatiles (C–H–O) are present in the rocks. The presence of volatiles lowers the solidus by 300°–500 °C below ca. 90 km depth compared to dry rocks. Their presence further introduces a kink in the solidus (Wyllie, 1980) at this depth, which may explain why significant LVLs are rarely identified at shallower depths.

The present study confirms the existence of a low velocity layer in the upper mantle below a depth of about 100 km in Siberia, although not fully compelling. Our result is based on non-linear inversion of surface wave dispersion curves, which may provide some of the best constraints for the detection of a mantle low velocity layer. However, we also find that the LVL needs to be pronounced in order to be unambiguously identified.

Acknowledgements

We are grateful to G. Laske and G. F. Panza for their very fruitful comments. We wish to thank two anonymous reviewers for very instructive comments that helped to improve the manuscript. The Carlsberg Foundation and the Danish Natural Science Research Foundation funded this research project.

References

Abramovitz, T., Thybo, H., Perchuc, E., 2002. Tomographic inversion of seismic P- and S-wave velocities from the Baltic Shield based on FENNOLORA data. Tectonophysics 358, 151–174.

Artemieva, I.M., Mooney, W.D., 2001. Thermal thickness and evolution of Precambrian lithosphere: a global study. J. Geophys. Res. 106 (B8), 16387–16414.

Ben-Menahem, A., Singh, S.J., 2000. Seismic Waves and Sources. Dover Publ. Inc, Mineola, New York.

Biswas, N.N., Knopoff, L., 1974. The structure of the upper mantle under the U.S. from the dispersion of Rayleigh waves. Geophys. J. R. Astron. Soc. 36, 515–539.

Bolt, B.A., Dorman, J., 1961. Phase and group velocity of Rayleigh waves in spherical gravitating earth. J. Geophys. Res. 66, 2965–2981.

Brune, J., Dorman, J., 1963. Seismic waves and earth structure in the Canadian Shield. Bull. Seismol. Soc. Am. 53, 167–209.

Egorkin, A.V., 1991. Crustal structure from seismic long-range profiles. In: Beloussov, V.V., Pavlenkova, N.I., Kvjatkovskaja, G.N. (Eds.), Deep Structure of the URSS Territory. Nauka, Moscow, pp. 118–135.

Ekstrom, G., Tromp, J., Larson, E.W.F., 1997. Measurements and global models of surface waves propagation. J. Geophys. Res. 102, 8137–8157.

Florsch, N., Fäh, D., Suhadolc, P., Panza, G.F., 1991. Complete synthetic seismograms for high-frequency multimode SH-waves. Pure Appl. Geophys. 136, 529–560.

Fowler, C.M.R., 1995. The Solid Earth. An Introduction to Global Geophysics. Cambridge Univ. Press.

Hales, A.L., 1991. Upper mantle models and the thickness of the continental lithosphere. Geophys. J. Int. 105, 355–363.

Herak, M., Panza, G.F., Costa, G., 2001. Theoretical and observed depth correction for M_s. Pure Appl. Geophys. 158, 1517–1530.

Kennett, B.L.N., Engdahl, E.R., 1991. Travel times for global earthquake location and phase identification. Geophys. J. Int. 105, 429–465.

Knopoff, L., 1972. Observation and inversion of surface-wave dispersion. Tectonophysics 13 (1–4), 497–519.

Kovach, R.L., Anderson, D.L., 1962. Long-period Love waves in a heterogeneous spherical earth. J. Geophys. Res. 67 (13), 5243–5255.

Kovach, R.L., Anderson, D.L., 1964. Higher mode surface waves and their bearing on the structure of the earth's mantle. Bull. Seismol. Soc. Am. 54 (1), 161–182.

Levshin, A.L., Pisarenko, V.F., Pogrebinsky, G.A., 1972. On a frequency time analysis of oscillations. Ann. Geophys. 28, 211–218.

Levshin, A.L., Ratnikova, L., Berger, J., 1992. Peculiarities of surface wave propagation across Central Eurasia. Bull. Seismol. Soc. Am. 82, 2464–2493.

Levshin, A.L., Ritzwoller, M.H., Ratnikova, L.I., 1994. The nature and cause of polarization anomalies of surface waves crossing northern and central Eurasia. Geophys. J. Int. 117, 557–590.

Ludwig, W.J., Nafe, J.E., Drake, C.L., 1970. Seismic Refraction. The Sea Vol. 4: Part 1. Wiley-Intersci, New York, pp. 53–84.

Muller, G., 1985. The reflectivity method: a tutorial. J. Geophys. 58, 153–174.

Nielsen, L., Thybo, H., Solodilov, L., 1999. Seismic tomographic inversion of Russian PNE data along profile Kraton. Geophys. Res. Lett. 26 (22), 3413–3416.

Nielsen, L., Thybo, H., Egorkin, A.V., 2001. Constraints on reflective bodies below the 8° discontinuity from reflectivity modelling. Geophys. J. Int. 145, 759–770.

Nielsen, L., Thybo, H., Egorkin, A.V., 2002. Implications of seismic scattering below the 8° discontinuity along PNE profile Kraton. Tectonophysics 358, 135–150.

Panza, G.F., 1981. The resolving power of seismic surface waves with respect to crust and upper mantle structural models. In: Cassinis, R. (Ed.), The Solution of the Inverse Problem in Geophysical Interpretation. Plenum Publ. Corp, pp. 39–77.

Panza, G.F., 1985. Synthetic seismograms: the Rayleigh waves modal summation. J. Geophys. 58, 125–145.

Panza, G.F., Calcagnile, G., 1974a. Comparison of the multimode surface wave response in structures with and without a low velocity channel: Part I. Dip–slip sources on a vertical fault plane. Pure Appl. Geophys. 112, 583–596.

Panza, G.F., Calcagnile, G., 1974b. Comparison of the multimode surface wave response in structures with and without a low velocity channel: Part II. Dip–slip sources. Pure Appl. Geophys. 112, 1031–1043.

Panza, G.F., Calcagnile, G., 1975. Comparison of the multimode surface wave response in structures with and without a low velocity channel: Part III. Strike–slip sources. Pure Appl. Geophys. 113, 661–671.

Panza, G.F., Suhadolc, P., 1987. Complete strong motion synthetics. In: Bolt, B.A. (Ed.), Seismic Strong Motion Synthetics. Academic Press, Orlando, pp. 153–204.

Panza, G.F., Schwab, F.A., Knopoff, L., 1973. Multimode surface waves for selected focal mechanism: I. Dip–slip sources on a vertical fault plane. Geophys. J. R. Astron. Soc. 34, 265–278.

Pavlenkova, N.I., 1996. General features of the upper mantle stratification from the long-range seismic profiles. Tectonophysics 264, 261–278.

Pavlenkova, G.A., Priestley, K., Cipar, J., 2002. 2D model of the crust and uppermost mantle along Rift profile, Siberian craton. Tectonophysics 355, 171–186.

Perchuc, E., Thybo, H., 1996. A new model of upper mantle P-wave velocity below the Baltic Shield: indication of partial melt in the 95 to 160 km depth range. Tectonophysics 253, 227–245.

Priestley, K., Debayle, E., 2003. Seismic evidence for a moderately thick lithosphere beneath the Siberian Platform. Geophys. Res. Lett. 30 (3), 1118.

Ritzwoller, M.H., Shapiro, N.M., Barmin, M.P., Levshin, A., 2002. Global surface wave diffraction tomography. J. Geophys. Res. 107 (B12), 2335.

Rodi, W., Glover, P., Li, T.M.C., Alexander, S.S., 1975. A fast, accurate method for computing group-velocity partial derivatives for Rayleigh and Love waves. Bull. Seismol. Soc. Am. 65 (5), 1105–1114.

Sato, H., Sacks, I.S., Murase, T., 1989. The use of laboratory velocity data for estimating temperature and partial melt fraction in the low-velocity zone: comparison with heat flow and electrical conductivity studies. J. Geophys. Res. 94 (B5), 5689–5704.

Shapiro, N.M., Ritzwoller, M.H., 2002. Monte-Carlo inversion for a global shear-velocity model of the crust and upper mantle. Geophys. J. Int. 151, 88–105.

Shearer, P.M., 1999. Introduction to Seismology. Cambridge University Press.

Thybo, H., Perchuc, E., 1997. The seismic 8 degree discontinuity and partial melting in the continental mantle. Science 275, 1626–1629.

Trampert, J., Woodhouse, J.H., 1995. Global phase velocity maps of Love and Rayleigh waves between 40 and 150 s period. Geophys. J. Int. 122, 675–690.

Urban, L., Cichowicz, A., Vaccari, F., 1993. Computation of analytical partial derivatives of phase and group velocities for Rayleigh waves with respect to structural parameters. Stud. Geophys. Geod. 37, 14–36.

Valyus, V.P., 1972. Determining seismic profiles from a set of observations. In: Keilis-Borok, I. (Ed.), Computational Seismology. Consult. Bureau, New York, pp. 114–118.

Valyus, V.P., Keilis-Borok, V.I., Levshin, A., 1969. Determination of the upper-mantle velocity cross-section for Europe. Proc. Acad. Sci. USSR 185 (3).

van Heijst, H.J., Snieder, R., Nowack, R., 1994. Resolving a low-velocity zone with surface-wave data. Geophys. J. Int. 118, 333–343.

Woodhouse, J.H., 1988. The calculation of eigenfrequencies and eigenfunctions of the free oscillations of the earth and the sun. In: Doornbos, D.J. (Ed.), Seismological Algorithms, Computational Methods and Computer Programs. Academic Press, London, pp. 321–370.

Wyllie, P.J., 1980. The origin of Kimberlite. J. Geophys. Res. 85 (B12), 6902–6910.

Yanovskaya, T.B., Kozhevnikov, V.M., 2003. 3D S-wave velocity pattern in the upper mantle beneath the continent of Asia from Rayleigh wave data. Phys. Earth Planet. Inter. 138, 263–278.

Yanovskaya, T.B., Antonova, L.M., Kozhevnikov, V.M., 2000. Lateral variations of the upper mantle structure in Eurasia from group velocities of surface waves. Phys. Earth Planet. Inter. 122, 19–32.